J. Chem. Soc., Faraday Trans. 2, 1983, **79**, 137–151

Far-infrared and Computer-simulation Analysis of Liquid and Rotator-phase Bromoform

BY VINOD K. AGARWAL,† GARETH J. EVANS AND MYRON W. EVANS*

Edward Davies Chemical Laboratories, The University College of Wales, Aberystwyth SY23 1NE

Received 2nd June, 1982

The existence of a liquid-to-rotator phase transition in bromoform is confirmed by far-infrared interferometric and laser spectroscopy. The molecular dynamics of liquid bromoform a few degrees above the melting point are simulated by computer and a variety of spectral data produced for comparison with experimental indications. It is easier to reproduce "single-molecule" infrared, Raman and n.m.r. correlation times than those from "multi-molecule" sources such as dielectric, far-infrared and Rayleigh-scattering spectroscopy. The computer simulation shows that roatation is nearly completely decoupled from translation in liquid and rotator-phase bromoform a few degrees above and below the phase transition, respectively. There is strikingly less rotation–translation coupling than in CH_3CN for example, a more elongated and dipolar molecule with the same C_{3v} symmetry which does not form a rotator phase.

Bromoform is a molecular liquid whose dynamical properties have been the subject of investigation in several different fields. These include dielectric[1] and far-infrared[2] spectroscopy, Raman[3–8] and Rayleigh scattering,[3] infrared bandshape analysis[4,8] and n.m.r. relaxation. A short review of the results is given by Brodbeck *et al.*[8] The liquid freezes at 281 K to a rotator (γ) phase, as reported by Agarwal *et al.*[9]

Despite the individual efforts of a number of research groups, the collected correlation times[8] of Brodbeck *et al.* do not give a clear idea of the nature of the molecular dynamics in $CHBr_3$ liquid. Indeed there is considerable disagreement, which extends even to the seemingly simple matter of definition of "correlation time". Brodbeck *et al.*[8] notice that literature correlation times may *double* according to definition, so that the results of individual papers may not be directly comparable. For example, Boldeskul *et al.*[7] define the correlation time as the time taken by the normalised autocorrelation function (a.c.f.) in question to fall to 1/e. Other authors use the bandwidth $\Delta\omega$ to calculate the relaxation time as $\tau \propto \Delta\omega^{-1}$. (This is the method used by Brodbeck *et al.*[8] themselves.) Others use the zeroth moment of the particular orientational autocorrelation function under question.

Part of the purpose of this paper is to attempt to pull these threads of evidence into order using the theoretical technique of computer simulation[10] to reproduce all the relevant experimentally derived autocorrelation functions from a model of the intermolecular effective-pair potential. The true potential of interaction between two bromoform molecules has not yet been derived experimentally, and in any case this would not be appropriate in the liquid, where molecular interaction potentials do not add up pairwise.[11] To deal with the second problem, computer simulation algorithms use effective-pair potentials to try to account for the effect of neighbours on a given pair of molecules. The modelling of the pair potential itself contains an element of subjectivity. In order to reduce this to a minimum it

† On leave from Department of Physics, Meerut University, Meerut, India.

seems to us that the "atom–atom Lennard-Jones + charges" framework[10,11] is a sound one upon which to attempt a construction of the available dynamical data (spectra of various kinds) from the available intermolecular potential parameters. Moreover, it is advantageous to adopt atom–atom Lennard-Jones and charge parameters as independently given in the literature. These should be used directly in the computer simulation without adjustment. It is then clear that the computation is based on a *model* of the intermolecular potential. The resulting computed a.c.f. are internally consistent, and it is possible to use them to pick out serious inconsistencies in the experimental data. We have demonstrated this technique already[12,13] for liquid CH_2Cl_2 and $CHCl_3$. In simulating all three liquids we have kept to the *same* (literature) Lennard-Jones parameters for C and H, and have based our calculation of partial charges on the very simple l.c.a.o. (linear combination of atomic orbitals) technique developed by del Re.[14]

It is always true that such simple (but not crude) estimates of the intermolecular potential may be refined. Two very sensitive aids to achieving this goal are vapour-phase second dielectric virial measurements[11,15] (for the pair potential) and the liquid-phase far-infrared spectrum.[10] The latter is a reflection of multi-body dynamics and liquid bromoform at 298 K is reported in the literature[2] to peak at 37 cm^{-1}, with a maximum power absorption of only 8 neper cm^{-1}. The half-width of the spectrum is 49 cm^{-1}. The far-infrared integrated absorption intensity is the second moment of the dielectric loss curve, which peaks at a lower frequency, corresponding to the inverse of the dielectric relaxation time, measured by Soussen–Jacob *et al.*[1] at 19.0 ps. If one does not involve polarisability in the model pair potential (we do not) then it is not possible to reproduce the well known features of far-infrared *collision-induced* absorption.[10] Comparison of the measured and simulated far-infrared bandshapes (on a reduced scale) will immediately bring out fresh information on the role of collision induction in liquid $CHBr_3$. Yet more information will become available by repeating this procedure in the rotator phase,[9] where we expect (*a priori*) the environmental symmetry to reduce the effect of collision induction, so that a greater degree of similarity might be expected between the measured and computed far-infrared spectra. In order to test this we have carefully measured, for the first time, the far-infrared spectrum of $CHBr_3$ in the rotator phase by interferometric techniques and using a new far-infrared laser system. This is the second moment spectrum of a dielectric loss curve which has been characterised by Agarwal *et al.*[9] in the kHz region. The *complete* kHz–THz (far-infrared) frequency region is the correct entity for analysis in the rotator phase.

With, then, a relatively simple model for $CHBr_3$ interaction we aim to assess the available literature correlation times for consistency, using the far-infrared spectrum as a sensitive measure of the effectiveness of the computer simulation.

EXPERIMENTAL

The far-infrared power-absorption spectra of liquid and rotator-phase bromoform were measured using two independent instruments. The broad-band spectrum was measured with a Grubb–Parsons/N.P.L. "Cube" interferometer. These data were checked for absolute intensity with an Apollo Instruments submillimetre laser, tunable over far-infrared lines of methanol vapour, pumped by a CO_2 laser source. This instrument produces spot-frequency values of power absorption and accurately fixes the absolute intensity, an important consideration when dealing with the effects of collision-induced absorption. The spectra, from both methods, are illustrated in fig. 1 for bromoform in the liquid and rotator phases. The rotator-phase spectrum is shifted slightly to higher frequencies. The bandshapes are compared directly in a reduced (or normalised) scale in fig. 2. Following the approach commonly

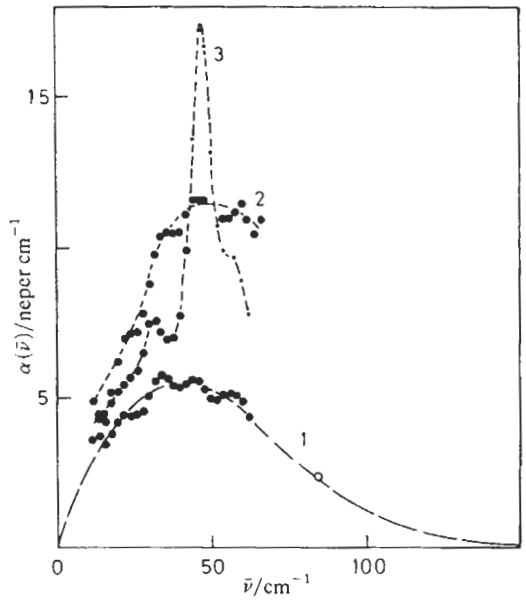

FIG. 1.—Power absorption of bromoform in (1) the liquid phase at 295 K, ○ laser point; (2) the rotator phase at 273 K; (3) the crystalline solid.

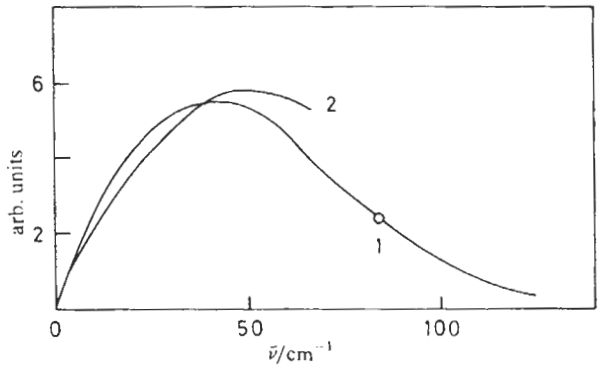

FIG. 2.—Liquid (1) and rotator-phase (2) spectra normalised to the same peak power absorption.

used in dielectric studies we have used single spot frequencies from our far-infrared laser to record changes in the spectra as a function of temperature. We also report interferometric results for $CHBr_3$ in the solid state when phonon modes are clearly resolved. These are not present in the temperature region (−2–+8 °C) where Agarwal *et al.*[9] have postulated the existence of a solid rotator-phase state. We believe our results firmly substantiate the existence of such.

THEORETICAL

COMPUTER SIMULATION

The algorithm used to simulate the motion and interaction of 108 $CHBr_3$ molecules was developed to integrate the rotational and translational equations of

motion with basically the same numerical method. The integration of the rotational equations of motion is slightly the more complicated and is based on a fourth-order predictor method for the angular momentum $\boldsymbol{J}$.

The interaction between $CHBr_3$ molecules is modelled by a 5×5 atom–atom Lennard-Jones "core" with point charges localised at each atomic site. The Lennard-Jones parameters are as follows: $\sigma(H—H) = 2.75$ Å; $\sigma(Cl—Cl) = 3.50$ Å; $\sigma(C—C) = 3.20$ Å; $\varepsilon/k(H—H) = 13.4$ K; $\varepsilon/k(Br—Br) = 263.0$ K; $\sigma(Br—Br) = 3.7$ Å. The H and C parameters are identical to those used in a simulation of liquid chloroform, reported elsewhere. The parameters for Br were taken from literature values by Eliel *et al.*[16] which are apparently successful in reproducing crystal-phase properties such as heat of sublimation. The partial charges used for bromoform were calculated on the basis of an estimate for chloroform by del Re.[14] Taking into account the slightly smaller dipole moment of $CHBr_3$ in comparison with $CHCl_3$, the increase in bond length from C—Cl to C—Br and the slightly smaller electronegativity of Br in comparison with Cl we arrive at the following estimate of partial charges for $CHBr_3$: $q_H = 0.021|e|$; $q_c = 0.055|e|$; $q_{Br} = -0.059|e|$. Our $CHBr_3$ pair potential is therefore modelled on independent literature estimates of the parameters involved. Lorentz–Berthelot combining rules were used to calculate cross-terms where appropriate.

The simulation run was initiated at 293 K, with a molar volume of 87.5 cm^3. We used 108 molecules, which were initially arranged on a face-centred cubic lattice in a cube of half-side 12.5 Å (the potential cut-off distance), which is over three times the largest σ of the Lennard-Jones and electrostatic interactions. For Lennard-Jones interactions atomic sites were considered independently of which molecules they belonged to. The electrostatic interaction was considered as a molecular property, and the minimum image convention and cut-off criterion were applied to the centre-of-mass–centre-of-mass distance, accounting for all 25 contributions for each pair of molecules. For relatively small partial charges (as in $CHBr_3$) there is apparently no need for an elaborate correction for long-range electrostatic forces, such as the Ewald sum method, because the dominant forces are those from the Lennard-Jones core.

INTEGRATION SCHEME FOR THE EQUATIONS OF MOTION

TRANSLATION

The translational motion of each molecule's centre of mass was integrated with the two-step Verlet algorithm:

$$R_i(t+\Delta t) = 2R_i(t) - R_i(t-\Delta t) + \frac{\Delta t^2}{M} F_i(t) + \mathcal{O}(\Delta t^4)$$

with $F_i(t)$ the total force on molecule i and M the total mass of the molecule. Velocities are computed with an uncertainty of $\mathcal{O}(\Delta t^3)$.

ROTATION

Rotational equations of motion are integrated in two stages. Once the total torque $N_i(t)$ has been computed from atomic forces, the angluar momentum $\boldsymbol{J}$ at time t is computed with

$$J_i(t) = J_i(t-\Delta t) + \int_{t-\Delta t}^{t} N_i(t)\,\mathrm{d}t$$

where $N_i(t)$ is replaced by a cubic interpolation over its four previous values in time sequence. The accuracy in $J_i(t)$ is to order Δt^4.

The orientation of the $CHBr_3$ molecule is described by means of the coordinates in the laboratory frame of the intrinsic system of reference defined by the three unit vectors $\boldsymbol{e}_A$, $\boldsymbol{e}_B$ and $\boldsymbol{e}_C$ directed along the principal axes of the molecule. The equation of motion is the kinematic relation

$$\dot{e}_\alpha^{(i)} = \boldsymbol{\omega}_i \times \boldsymbol{e}_\alpha^{(i)}(t), \qquad \alpha = A, B, C$$

for each molecule i. Orthonormality is restored for each molecule in combination with a predictor algorithm which includes terms to order Δt^3.

Total energy is conserved to 1 part in 10^4 over segments of greater than a thousand time steps with fluctuation of the total kinetic energy of little less than 10%. On average, the equipartition between translation and rotation was well within 1%.

The results in this paper refer to a simulation of a system of 108 molecules in a box of side 12.52 Å ($V_m = 87.5\ cm^3\ mol^{-1}$) and a time step $\Delta t = 0.005$ ps. Equilibration took *ca.* 2000 steps for melting of the initial f.c.c. configuration, using an initial disturbance from a random number generator. The Verlet parameter $s(\boldsymbol{k}_x)$ for the centre of mass was monitored to follow the melting from the lattice configuration to the liquid. Long-range corrections to the virial sum and to the potential energy have been incorporated for the Lennard-Jones interaction only, because such sums diverge for the electrostatic contributions. This results in high values for the computed pressure.

AUTOCORRELATION FUNCTIONS

The molecular-dynamics algorithm can be used to compute a.c.f. from data stored on disk from an equilibrium run. These have been constructed by running time averaging, and are available for the following vectors:(i) $\boldsymbol{r}_{cm}$, the centre-of-mass position of each molecule; (ii) the centre-of-mass velocity $\boldsymbol{v}$; (iii) the three orientation vectors $\boldsymbol{e}_A$, $\boldsymbol{e}_B$ and $\boldsymbol{e}_C$; (iv) the molecular angular momentum, $\boldsymbol{J}$; (v) the force vector, $\boldsymbol{F}$, for each molecule; (vi) the molecular torque, $\boldsymbol{T}_q$; (vii) the rotational velocity vectors, $\dot{\boldsymbol{e}}_A$, $\dot{\boldsymbol{e}}_B$ and $\dot{\boldsymbol{e}}_C$ (relevant for far-infrared analysis); (viii) the molecular angular velocity, $\boldsymbol{\omega}$.

Autocorrelation functions may be computed in either the laboratory frame or in a rotating frame, which may be defined for convenience as that of the principal moments of inertia of the molecule. A considerable amount of information is therefore obtainable from a single molecular-dynamics run.

DEFINITION OF "CORRELATION TIMES"

In order to compare the results of the computer simulation with the values listed by Brodbeck *et al.*[8] we note our definition of "correlation time".

Bromoform is a C_{3v} symmetric top, with moments of inertia $I_A = 6.87 \times 10^{-28}$ gm cm^2, and $I_B = I_C = 1.352 \times 10^{-37}$ gm cm^2, as calculated from structural data using Hirschfelder's dyadic minimisation technique.[17] The dipole unit vector is $\boldsymbol{e}_A$. We define a first-rank orientational correlation time as the area beneath the a.c.f. $\langle \boldsymbol{e}_A(t) \cdot \boldsymbol{e}_A(0) \rangle$. The rotational a.c.f. derived from the ν_1(C—H) stretch of $CHBr_3$ in the infrared is also $\langle \boldsymbol{e}_A(t) \cdot \boldsymbol{e}_A(0) \rangle$ provided that the effects of vibration–rotation coupling can be eliminated correctly. According to Brodbeck *et al.*[8] this is possible. The Raman ν_1 stretch provides us with the rotational a.c.f.

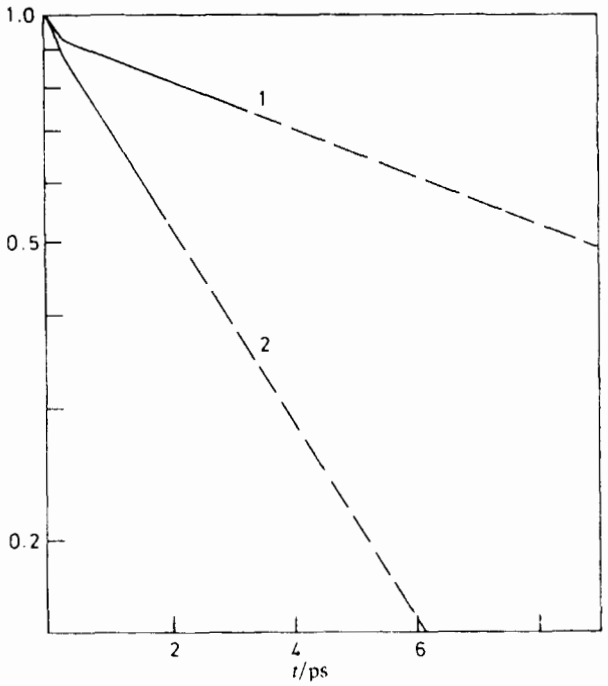

FIG. 3.—Computer-simulated normalised orientational a.c.f. for the dipole vector (e_A). (1) $P_1(e_A)$; (2) $P_2(e_A)$; $CHBr_3$ liquid, 293 K, 1 bar.

$\frac{1}{2}\langle 3[e_A(t) \cdot e_A(0)]^2 - 1\rangle$, which we can also simulate (fig. 3). We define the correlation time of this a.c.f. as the area beneath it (when normalised) in the interval $t = 0$ to $t = \infty$. In principle this can be obtained also from n.m.r. dipole–dipole relaxation, as discussed by Farrar *et al.*[18] and Sandhu.[19] (The dipole–dipole ^{13}C n.m.r. relaxation time refers to the ^1H to ^{13}C vector of $CHBr_3$, which is directionally the same as e_A.) Sandhu[19] has separated the contributions of spin-rotation and inter- and intra-molecular dipole–dipole relaxation in liquid $CHBr_3$, and in general all three contribute to the observable nuclear spin relaxation.

From the intermolecular dipole–dipole relaxation Sandhu calculates a translational correlation time of 10.4 ps at 298 K, making some assumptions in the data reduction. One of these is that the diffusion tensor is related to the effective molecular radius by Stokes' law.

From the intramolecular dipole–dipole relaxation a rotational (P_2) correlation time of 4.1 ps is calculated at 293 K. However, the data reduction assumes that the rotational diffusion is isotropic, and also uses a microviscosity correction factor on empirical grounds. The n.m.r. correlation time of Sandhu is clearly much less than 1/3 of the dielectric (P_1) relaxation time measured by Soussen-Jacob *et al.*[1] (19 ps), and recently remeasured by Sharma and Agarwal[20] as 24.4 ps at 293 K, rapidly decreasing to 13.3 ps at 323 K. This is inconsistent with the theory of rotational diffusion used by all three sources in deriving these rotational correlation times. A computer simulation produces self-consistent correlation times for a given model of the intermolecular effective-pair potential, and will help interpret the experimental literature.

The *multimolecular* counterparts of $\langle e_A(t) \cdot e_A(0)\rangle$ and $\frac{1}{2}\langle 3[e_A(t) \cdot e(0)]^2 - 1\rangle$ are obtainable from dielectric relaxation and depolarised Rayleigh scattering, respectively. These cross-correlation functions involve all the molecules in the sample and are much more difficult to simulate. In this paper we have attempted an estimate of these functions using correlation built up between small sub-spheres containing three or four $CHBr_3$ molecules. The evidence provided by Brodbeck *et al.*[8] seems to indicate that the correlation times involved in cross-correlation are longer than those of the a.c.f. For example, the dielectric relaxation time, measured by Soussen-Jacob *et al.*,[1] is 19 ps, and the infrared rotational correlation time (Brodbeck *et al.*) is either 4.1 or 8.2 ps, according to definition. The ν_1 stretch Raman correlation times from various sources fall in the range 2.0–5.1 ps, and the depolarised Rayleigh correlation time of Patterson and Griffith[3] is 10.1 ps. In this paper our definition of "correlation time" for the cross-correlation functions is the same as that for the a.c.f.: the area beneath the normalised correlation function in the interval $t = 0$ to $t = \infty$.

Finally in this section we note that the far-infrared spectrum is also a multimolecular property, being essentially the second-moment of the dielectric loss. The "auto" part of the complete correlation function is the rotational velocity a.c.f. $\langle \dot{e}_A(t) \cdot \dot{e}_A(0)\rangle$, which can be simulated straightforwardly. The direct Fourier transform of this a.c.f. provides us with the equivalent "auto" far-infrared spectrum. The *measured* far-infrared spectrum is a Fourier transform of the complete rotational velocity cross-correlation function, after allowance has been made for the internal field effects which are always present in a liquid. We have attempted to construct this spectrum in this paper using sub-spheres, as mentioned earlier.

RESULTS AND DISCUSSION

Fig. 1 shows the spectra recorded by the interfometric technique for liquid bromoform at 295 K, bromoform in the solid state at 275 K and bromoform in the solid state at 265 K. In the solid state a broad band exists akin to that of the liquid although of increased intensity and shifted slightly to higher frequencies. No sharp phonon modes, characteristic of the far-infrared spectra of a solid, are present, although they do emerge below the dipole melting point (271 K) reported by Agarwal *et al.*[9] We believe these spectra provide strong further evidence for the existence of a solid rotator phase. In fig. 2 we show the liquid and rotator-phase spectra normalised to the same peak power absorption to emphasize the differences and similarities that exist. In fig. 1 and 2 we show a laser point for comparison with the interferometric results at 84 cm^{-1}. All the data agree well. We have also used the laser to follow changes in the spectra as a function of temperature, a technique more commonly used in dielectric spectroscopy. One such run is shown later in fig. 10, where the phase change from liquid to solid rotator phase is clearly discerned as the change in the slope. This method of monitoring phase changes is to be the subject of further research that will be reported elsewhere.

In table 1 we compare some of the simulated correlation times with results from the various experimental sources. The agreement is satisfactory for the "single-particle" infrared and Raman correlation times. The infrared (C—H stretch), rotational correlation time, for example, is 8.2 ± 3.3 ps compared with a computer simulated time of 11.0 ps. [This is the area beneath the simulated dipole vector autocorrelation function $\langle e_A(t) \cdot e_A(0)\rangle$, fig. 3.] There is satisfactory agreement between the n.m.r. μ–μ (rotational) mean correlation time derived by Sandhu[19] and the three computer-simulated correlation times: the areas beneath

TABLE 1.—COMPARISON OF EXPERIMENTAL AND COMPUTER-SIMULATED CORRELATION TIMES FOR LIQUID BROMOFORM[a]

technique	correlation time/ps	simulation: autocorrelation time/ps
dielectric relaxation	19.0[1,20]	11.0 (e_A)
infrared ν_1 stretch (C—H)	8.2 ± 3.3[8]	11.0 (e_A)
Raman ν_1 stretch (C—H)	5.1 ± 1.0[8] 2.0 (1/e)[7] 3.1[5] 4.4[3]	2.8 (e_A)
Raman ν_2, (CBr_3 sym. stretch)	3.4[7] 4.4[5]	weighted mean of: 2.8 (e_A), 4.5 (e_B, e_C)
Raman ν_3, (CBr_3 symm. bend)	5.3[6] 6.8[7] 6.6[5]	4.5 (e_B, e_C)
Rayleigh scattering	10.1[3]	weighted mean of: 2.8 (e_A), 4.5 (e_B, e_C)
n.m.r. intramolecular μ–μ	4.1[19] (average)	weighted mean of: 2.8 (e_A), 4.5 (e_B, e_C)
intermolecular μ–μ translational correlation time	$\tau_c = 10.4$[19]	$\tau_v < 0.1$[b] $\tau_t \approx 11.3$

[a] In the rotator phase at 273 K, $\tau_1(e_A)$ (first rank) is 18.0 ps and $\tau_2(e_A)$ (second rank) is 5.7 ps from the computer simulation (see Appendix), [b] Centre-of-mass velocity.

$P_2(e_A)$, $P_2(e_B)$ and $P_2(e_C)$, respectively. However, there is a serious discrepancy between the intermolecular μ–μ n.m.r. (translational) correlation time of 10.4 ps and the computer simulated value, <0.1 ps, (see fig. 4). The referees have kindly made the following points in this context. (i) If the motion were describable by the diffusion equation and an exponentially decaying $\langle \boldsymbol{v}(t) \cdot \boldsymbol{v}(0) \rangle$ then the $(\tau_c)_{trans}$ which occurs in Sandhu [ref. (19), eqn (10)] would be

$$\tau_c = \frac{a^2}{12D} = \frac{ma^2}{12kT\tau_v}$$

where a is the molecular radius,[19] m the molecular mass and τ_v velocity correlation time. Therefore we must correct τ_v of the molecular dynamics simulation (table 1) and relate it to the measured τ_c as above. Assuming a molecular radius of 3.6 Å and using the molecular mass we obtained a "simulated" τ_c of 11.3 ps. (ii) Sandhu assumes Stokes' law specifically for comparison with calculated values of $1/T_1$. For the data reduction he uses his eqn (10), for which he has to assume values of the molecular radius a and the distances of closest approach d_{HH} and d_{HBr}. The values of these parameters do not seem to be reported.[19] The computer simulated centre-of-mass velocity autocorrelation function, $\langle \boldsymbol{v}(t) \cdot \boldsymbol{v}(0) \rangle / \langle v^2(0) \rangle$, is not exponential, as assumed by Sandhu in his derivation,[19] and has the characteristic, long negative tail. The second-moment a.c.f. $\langle \boldsymbol{v}(t) \cdot \boldsymbol{v}(t)\boldsymbol{v}(0) \cdot \boldsymbol{v}(0) \rangle / \langle v^4(0) \rangle$ goes to

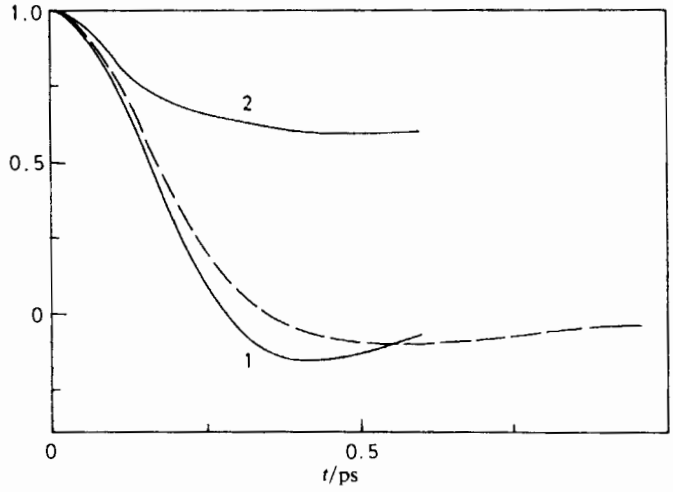

FIG. 4.—Centre-of-mass velocity a.c.f. for $CHBr_3$, computer simulated; 293 K, 1 bar. (1) $\langle \boldsymbol{v}(t) \cdot \boldsymbol{v}(0) \rangle / \langle \boldsymbol{v}^2(0) \rangle$, (2) $\langle \boldsymbol{v}(t) \cdot \boldsymbol{v}(t)\boldsymbol{v}(0) \cdot \boldsymbol{v}(0) \rangle / \langle v^4(0) \rangle$, (– – –) $\langle v_3(t)v_3(0) \rangle / \langle v_3^2(0) \rangle$, molecule fixed frame.

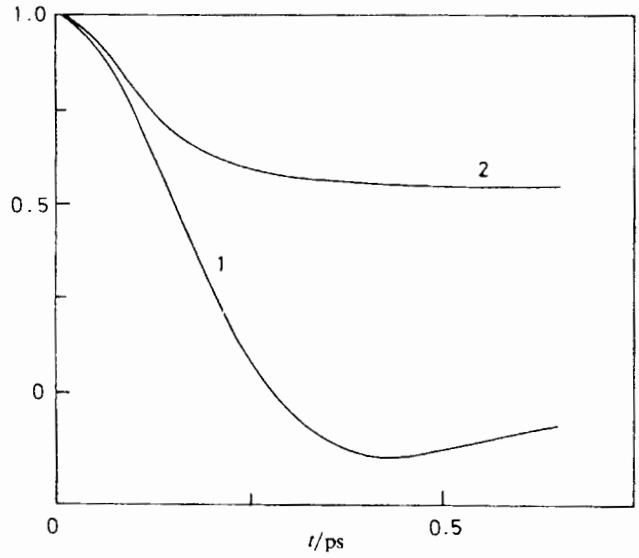

FIG. 5.—As for fig. 4, angular velocity a.c.f.

the Gaussian limit of 0.6 as $t \to \infty$ but is intermediately non-Gaussian. The angular momentum and angular velocity a.c.f. from the simulation (fig. 5) are similarly oscillatory, and decay in a similar time-scale to the centre-of-mass *linear* velocity a.c.f. This is strikingly corroborated in fig. 6, where the simulated force and torque a.c.f. behave identically in the interval up to 0.2 ps.

Agreement between simulation and experimental data is less satisfactory for dielectric relaxation, far-infrared absorption and depolarised Rayleigh scattering in liquid bromoform (table 1). Both the dielectric relaxation and Rayleigh correlation times are multi-molecular in origin and are only indirectly capable of providing

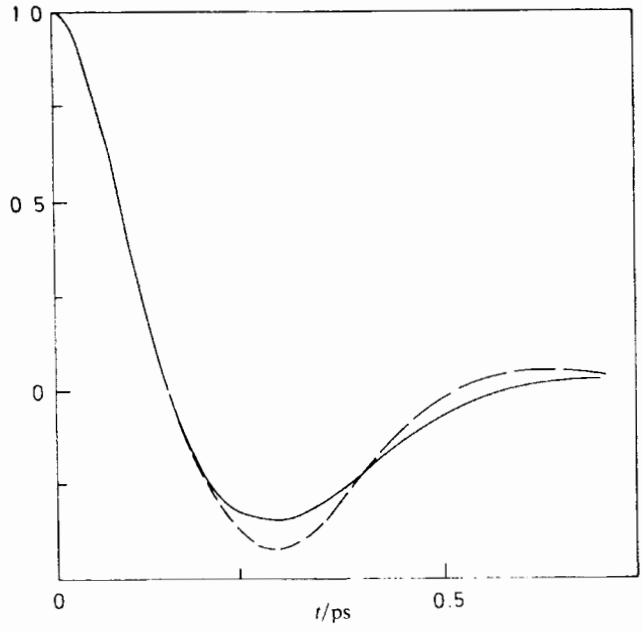

FIG. 6.—As for fig. 4, torque (——) and force (– – –) a.c.f.

information on *auto* correlation functions. This is further reflected in the discrepancy between the simulated rotational velocity a.c.f. (fig. 7) and the Fourier transform of the $\alpha(\bar{\nu})$ far-infrared power absorption of liquid bromoform as reported in this paper (fig. 1). However, it is interesting that Lund *et al.*[21] have made a direct comparison of the far-infrared spectrum of Jain and Walker[22] with their depolarised Rayleigh wing spectrum. If the intensity, $I(\bar{\nu})$, of the wing is multiplied by $|\bar{\nu}|[1-\exp(-\boldsymbol{h}|\bar{\nu}|\boldsymbol{kT})]$, where $\bar{\nu}$ is the wavenumber, the resulting "Rayleigh power spectrum" peaks at 35 cm^{-1}, in agreement with the maximum $\alpha(\bar{\nu})$ of Jain and Walker[22] (see table 1 of Lund *et al.*[21]). In fig. 7 we have used our remeasured spectrum (fig. 1) to calculate the experimental rotational velocity correlation function by Fourier transformation. This peaks at 40 cm^{-1}, 5 cm^{-1} higher in frequency than the values reported by Lund *et al.* If we used these latter spectra the experimental r.v.c.f. would be shifted by *ca.* 20% *towards* the computer simulated *auto* correlation function of fig. 7. It is clear, furthermore, that the experimental and simulated rotational velocity correlation functions are similar in shape. Also the $\alpha(\bar{\nu})$ and "Rayleigh power spectra" are shaped similarly. The integrated intensity of the far-infrared power coefficient is linear in number density of $CHBr_3$ molecules upon dilution (this work). These separate pieces of evidence all point to the conclusion that collision-induced phenomena are not significant in the far-infrared and depolarised Rayleigh wing spectra of liquid bromoform.

We have attempted to calculate the multimolecular rotational velocity correlation function for liquid bromoform, using sub-spheres, as reported elsewhere.[12,13] However, this method does not produce results significantly different from the computed correlation function of fig. 7.

The overall conclusion from the spectral analysis of the computer simulation is that some features are easier to reproduce in this way than others. The dielectric

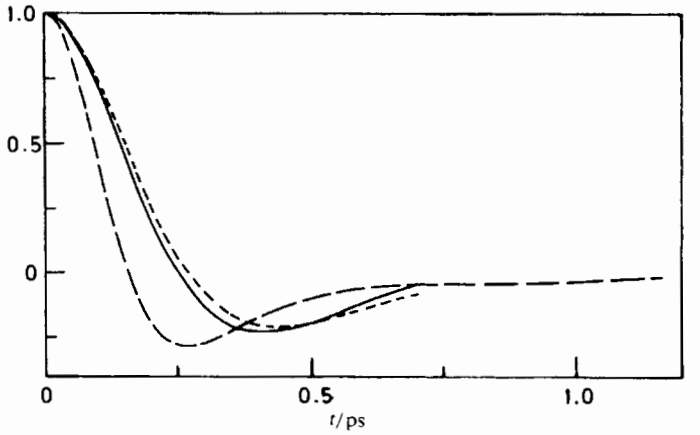

FIG. 7.—Rotational velocity correlation functions. Experimental (this work) (— —); simulations $\langle \dot{e}_A(t) \cdot \dot{e}_A(0) \rangle / \langle \dot{e}_A^2(0) \rangle$ (dipole vector, e_A) (——) and $\langle \dot{e}_C(t) \cdot \dot{e}_C(0) \rangle / \langle \dot{e}_C^2(0) \rangle$ (– – –).

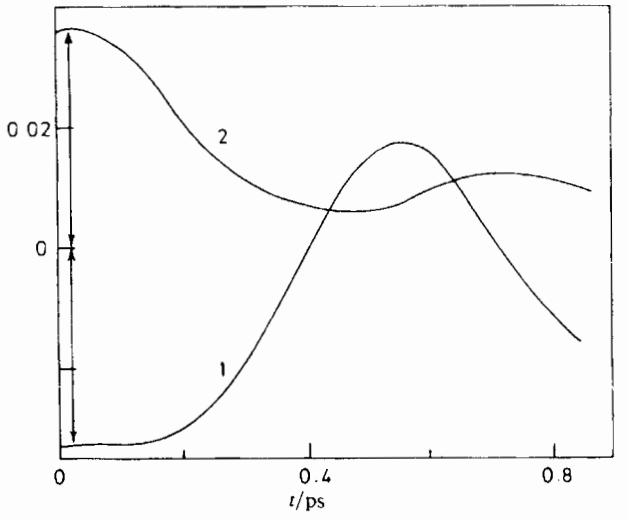

FIG. 8.—Rotation–translation a.c.f. $\langle \boldsymbol{v}(t) \boldsymbol{J}^T(0) \rangle$ in the moving frame. (1) 1, 2; (2) 2, 1 components. The noise level is indicated on the ordinate axis by the arrows. Functions are normalised by $\langle v_i^2 \rangle^{1/2} \langle J_i^2 \rangle^{1/2}$.

and far-infrared and depolarised Rayleigh wing spectra remain the most inaccessible, because they are multi-molecular properties. (A submillimetre measuring field in the far-infrared "sees" several thousand molecules at a time, and dielectric wavelengths extend over orders of magnitude more.) Therefore the computer simulation method is limited in its validity because we use only 108 molecules with periodic boundary conditions. The Raman, infrared and n.m.r. correlation times cluster fairly satisfactorily around the computer simulation results, except for the n.m.r. translational correlation time, which is very long in comparison with the area beneath $\langle \boldsymbol{v}(t) \cdot \boldsymbol{v}(0) \rangle / \langle v^2(0) \rangle$ from the simulation.

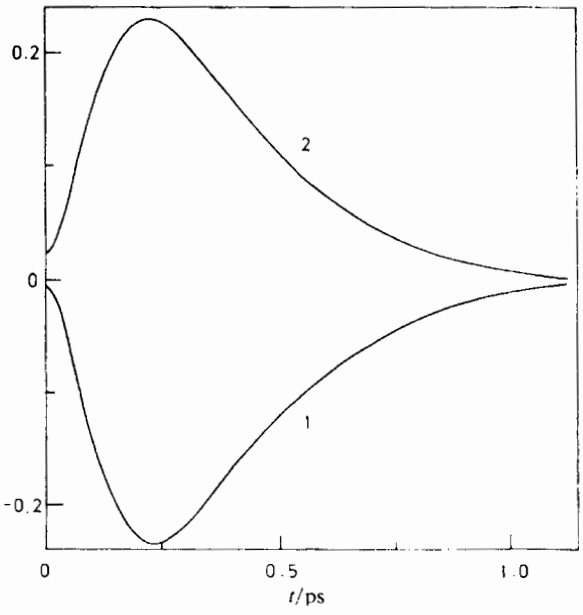

FIG. 9.—As for fig. 8, CH_3CN from a separate computer simulation. In this case the r/t coupling is much stronger for the same C_{3v} symmetry.

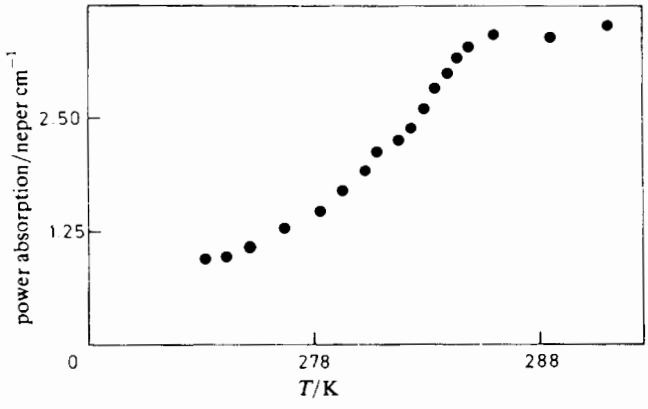

FIG. 10.—Laser spectroscopy of $CHBr_3$, plot of inverse power absorption at 84 cm^{-1} against temperature. The phase change is clearly discernible as a change in slope.

ROTATION–TRANSLATION COUPLING

Why does bromoform form a rotator phase? Part of the answer may be found in the dynamics of rotation–translation coupling. These may be discerned in a moving frame of reference, for convenience fixed in the principal moment of inertia frame of bromoform. If we transform the centre-of-mass velocity ($\boldsymbol{v}$) vector and molecular angular-momentum vector ($\boldsymbol{J}$) into the moving frame of reference and construct the elements of $\langle \boldsymbol{v}(t)\boldsymbol{J}^{\mathrm{T}}(0)\rangle$ the effect of rotation on translation is then observable directly.

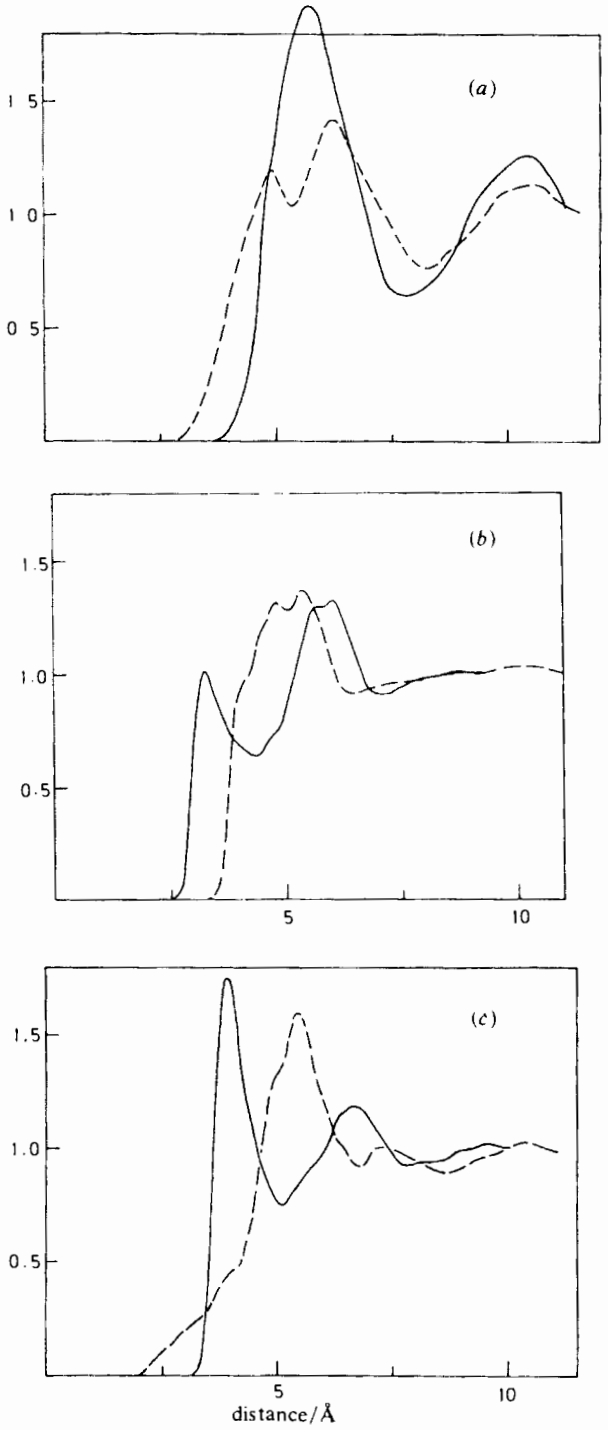

FIG. 11.—Atom–atom probability density functions for liquid bromoform at 293 K, computer simulation. (*a*) (——) C—C, (- - -) C—H; (*b*) (——) H—Br, (- - -) C—Br; (*c*) (——) Br—Br, (- - -) H—H.

By symmetry the only non-vanishing elements of the matrix $\langle \boldsymbol{v}(t)\boldsymbol{J}^{\mathrm{T}}(0)\rangle$ are (1, 2) and (2, 1). These are illustrated in fig. 8 and are both inside the noise limits of the simulation, *i.e.* are very small in magnitude. For comparison, we illustrate the same functions from a separate computer simulation of CH_3CN in fig. 9. In this case the rotation–translation coupling is much more pronounced for the same (C_{3v}) symmetry.

Therefore we have clear evidence from fig. 8 and 9 of one of the dynamical prerequisites for a rotator phase, rotation almost wholly uncoupled from translation.

ATOM–ATOM PAIR DISTRIBUTION FUNCTIONS

These are illustrated in fig. 11 for the various atom-to-atom pair distribution functions (p.d.f.) involved. The carbon to carbon p.d.f. of fig. 11(*a*) shows two clear peaks at 5.7 and 10.5 Å which are signatures of the position of the first and second shell of neighbours around a given bromoform molecule. The other atom to atom p.d.f. are more complicated in structure and reflect the probability of finding a given atom at a given distance from the reference atom on the same molecule or on a different molecule. A source of data for these functions would be incoherent inelastic neutron scattering carried out on different isotopes of C, H and Br. We defer further comment until these data are available.

The S.E.R.C. is acknowledged for financial support. Dr A. K. Agarwal and Dr M. Ferrario are thanked for fruitful discussions.

APPENDIX

A simulation of the rotator phase at 273 K produced the correlation times reported in the footnote to table 1. This was carried out with a molar volume of 82.8 cm^3, remeasured for this work with a pyknometer. The angular momentum and centre-of-mass linear velocity a.c.f. are oscillatory in the rotator phase and the rotation–translation coupling (fig. 8) is very small.

[1] J. Soussen-Jacob, E. Dervil and J. Vincent-Geisse, *Mol. Phys.*, 1974, **28**, 935.
[2] M. Benson, G. D. Martin, S. Walker, J. Warren and R. Wilson, *Can. J. Chem.*, 1972, **50**, 2610.
[3] G. D. Patterson and J. E. Griffiths, *J. Chem. Phys.*, 1975, **63**, 2406.
[4] A. Ruoff, I. Rossi-Sonnichsen, C. Brodbeck and Nguyen van Thanh, *C.R. Acad. Sci.*, 1974, **279**, 997.
[5] A. M. Amorin da Costa, M. A. Norman, and J. H. R. Clarke, *Mol. Phys.*, 1975, **29**, 191.
[6] F. J. Bartoli and T. A. Litovitz, *J. Chem. Phys.*, 1972, **56**, 413.
[7] A. E. Boldeskal, S. S. Esman and V. E. Pogornelov, *Opt. Spectrosc.*, 1974, **37**, 521.
[8] C. Brodbeck, I. Rossi, Nguyen van Thanh and A. Ruoff, *Mol. Phys.*, 1976, **32**, 71.
[9] V. K. Agarwal, A. K. Sharma and A. Mansingh, *Chem. Phys. Lett.*, 1979, **68**, 151.
[10] M. W. Evans, G. J. Evans, W. T. Coffey and P. Grigolini, *Molecular Dynamics* (Wiley-Interscience, New York, 1982), chap. 1.
[11] G. C. Maitland, M. Rigby, E. B. Smith and W. A. Wakeham, *Intermolecular Forces* (Oxford University Press, Oxford, 1980).
[12] M. W. Evans and M. Ferrario, *Chem. Phys.*, 1982, in press (parts 1 and 2).
[13] M. W. Evans, *Adv. Mol. Relaxation Processes*, 1982, in press.
[14] R. del Re. *J. Chem. Soc.*, 1958, 43.
[15] H. Sutter, in *Dielectric Relaxation and Molecular Processes* (The Chemical Society, London, 1972).
[16] E. K. Eliel, N. L. Allinger, S. J. Angyal and G. A. Morrison, *Conformational Analysis* (Wiley, New York, 1965).
[17] J. O. Hirschfelder, *J. Chem. Phys.*, 1940, **8**, 431.
[18] T. C. Farrar, S. J. Druck, R. R. Shoup and E. D. Becker, *J. Am. Chem. Soc.*, 1972, **94**, 699.

[19] H. S. Sandhu, *J. Magn. Reson.*, 1979, **34**, 141.
[20] A. K. Sharma and V. K. Agarwal, *Acta Chim. Acad. Sci. Hung.*, in press.
[21] P. A. Lund, O. Faurskov-Nielsen and E. Praestgaard, *Chem. Phys.*, 1978, **28**, 167.
[22] S. R. Jain and S. Walker, *J. Phys. Chem.*, 1971, **75**, 2942.

(PAPER 2/919)